

# Gouge fabrics reset by thermal pressurization record stress on faults after earthquakes

Li-Wei Kuo<sup>1,2\*</sup>, Hiroki Sone<sup>3</sup>, Vladimir Luzin<sup>4,5</sup>, En-Chao Yeh<sup>6</sup>, Ya-Ju Hsu<sup>7</sup> and Eh Tan<sup>7</sup>

<sup>1</sup>Department of Earth Sciences, National Central University, Taoyuan City 320, Taiwan

<sup>2</sup>Earthquake-Disaster & Risk Evaluation and Management Center, National Central University, Taoyuan City 320, Taiwan

<sup>3</sup>College of Engineering, University of Wisconsin-Madison, Madison, Wisconsin 53706, USA

<sup>4</sup>Australian Nuclear Science & Technology Organisation, Bragg Institute, Lucas Heights, NSW 2234, Australia

<sup>5</sup>School of Engineering, University of Newcastle, Callaghan, NSW 2308, Australia

<sup>6</sup>Department of Earth Sciences, National Taiwan Normal University, Taipei City 116, Taiwan

<sup>7</sup>Institute of Earth Sciences, Academia Sinica, Taipei City 115, Taiwan

## ABSTRACT

Stress on seismogenic faults provides critical information about how much elastic energy is stored in the crust and released by earthquakes, which is crucial in understanding earthquake energetics and recurrence. However, determining post-earthquake stress states on faults remains challenging because current borehole methods are rarely applicable to damaged fault zone rocks. We applied neutron texture analysis to gouge samples of the 1999 Chi-Chi earthquake in Taiwan to infer the stress state after the earthquake. Results indicate that the clay fabric within the principal slip zone is orthogonal to the fault plane, whereas outside the principal slip zone the fabric is predominantly parallel to the bedding-parallel fault plane. We suggest that the clay fabric in the slip zone was first neutralized by the coseismic fluidization caused by thermal pressurization and later re-oriented to the new direction of post-earthquake principal stress. Such stress orientation is consistent with the orientations inferred from core-scale fault slip data and dislocation models constrained from global navigation satellite system displacements. If thermal pressurization is a ubiquitous process during earthquakes, gouge fabrics can be used to help probe the post-earthquake stress state of faults.

## INTRODUCTION

Earthquakes result from the rapid release of stress accumulated on faults due to tectonic loading. Thus, the understanding of stress state on faults is of paramount importance for earthquake mechanics (Kanamori and Brodsky, 2004). Historically, the lack of heat flow anomaly at the San Andreas fault (California, USA; Lachenbruch and Sass, 1980) has sparked discussion about how fault shear strength inferred from laboratory rock mechanics experiments (~100 MPa; Byerlee, 1978) contradicts the apparent coseismic fault shear stress inferred from the thermal signals observed on active faults (~10 MPa; Kano et al., 2006). This apparent discrepancy has led to propositions about how major faults are weaker than the surrounding crust due to specific mineral assemblages (Lockner et al., 2011) and elevated pore fluid pressure (Faulkner and Rutter, 2001) and also

how faults are strong statically but temporarily weakened during dynamic fault slips (Sibson, 1973).

However, it remains unknown whether such explanations apply to all, or only a subset of, faults due to the scarcity of definitive observations of fault stress state before and after earthquakes. *In situ* subsurface stress states are commonly obtained by borehole-based methods such as hydraulic fracturing (Haimson and Fairhurst, 1969), observation of wellbore failures (Zoback et al., 2003), and anelastic strain recovery (ASR; Lin et al., 2006). But these methods are often difficult to apply to damaged rock masses found in active faults, or to obtain the true post-earthquake stress state on faults before they are disturbed by postseismic deformation because of the inevitable lag time between earthquakes and drilling penetration through fault zones.

We demonstrate a new approach for inferring fault stress states that is based on fabric

analysis of gouge samples recovered from the principal slip zone of an active fault. The method relies on the premise that (1) thermal pressurization resets the preexisting gouge fabric due to local fluidization, and (2) the gouge fabric re-orientates itself to align with the *in situ* stress, thereby recording the stress orientation at the fault plane right after an earthquake. The idea is validated by checking the consistency between the anomalous clay fabrics observed in fault gouge samples collected from the Chelungpu fault (Taiwan) and the inferred post-earthquake stress state at the location of the sample.

## CHELUNGPU FAULT

The Chelungpu thrust fault ruptured northward along an ~90 km segment as a result of the Mw 7.6 Chi-Chi earthquake on 21 September 1999 (Fig. 1A). The northern part of the fault segment was characterized by large displacement (8–10 m), high slip velocity (2–4 m/s), and a low level of high-frequency radiation (Ma et al., 2003). The low level of high-frequency radiation has been interpreted to be the result of several proposed dynamic fault weakening mechanisms, including elasto-hydrodynamic lubrication (Brodsky and Kanamori, 2001) and thermal pressurization (Tanikawa and Shimamoto, 2009).

The active fault zone of the Chi-Chi earthquake was drilled to a depth of 1137 m by the Taiwan Chelungpu Fault Drilling Project (TCDP) (described as core FZ1137 hereafter; Fig. 1B; Ma et al., 2006). The principal slip zone (PSZ) of the earthquake was identified from anomalous chemical (Ishikawa et al., 2008), magnetic (Chou et al., 2012), and mineralogical (Hirono et al., 2008) characteristics

\*E-mail: [liweikuo@ncu.edu.tw](mailto:liweikuo@ncu.edu.tw)

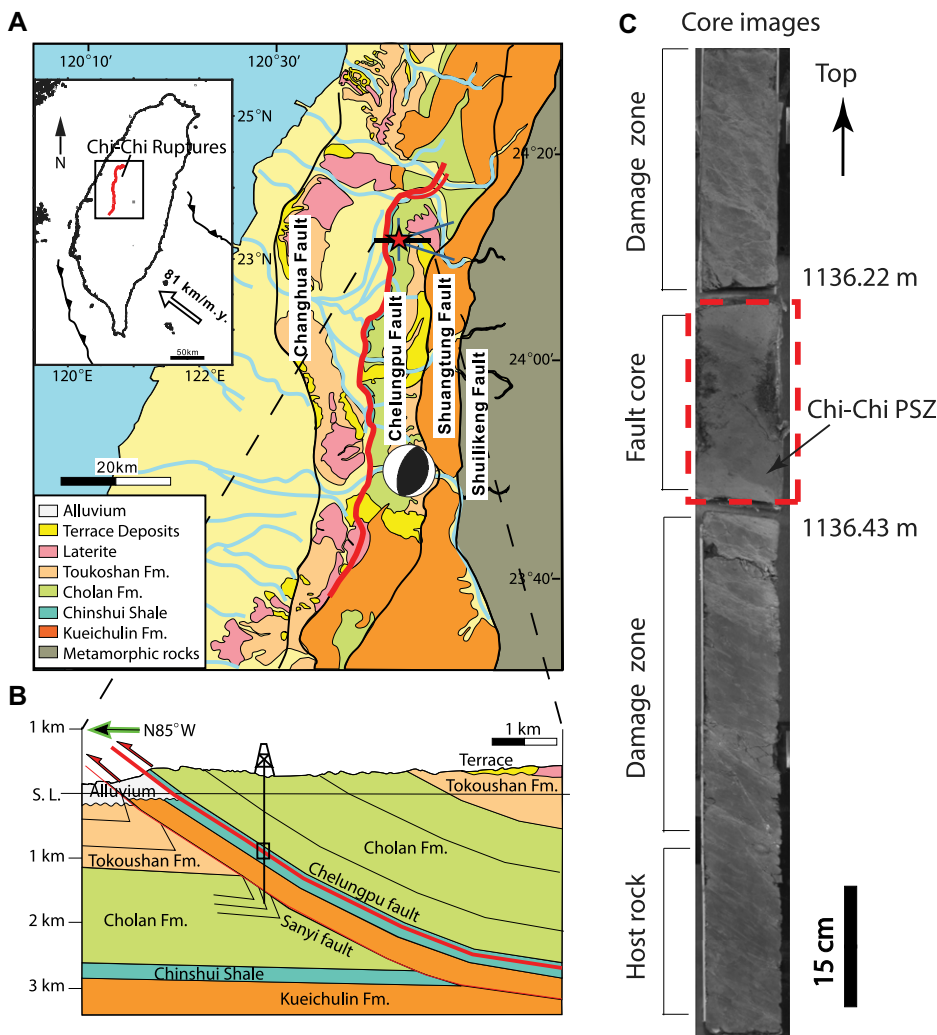


**Figure 1. Geological setting of the 1999 Mw 7.6 Chi-Chi earthquake in Taiwan and the Taiwan Chelungpu Fault Drilling Project (TCDP) borehole cores. (A) The 90-km-long surface ruptures associated with the Mw 7.6 earthquake in central Taiwan. Location of the TCDP site is indicated by a red star; the beach ball denotes the focal mechanism and the hypocenter of the Chi-Chi mainshock. Inset box shows the tectonic setting of Taiwan. Fm.—Formation. (B) An east-west cross section of the TCDP borehole showing the Chelungpu fault zone and surrounding formations encountered in the borehole. The black rectangle outlining the recognized active fault zone of the Chi-Chi mainshock is 1136 m deep. S.L.—surface level. (C) The major core of the Chelungpu fault viewed along the borehole of the TCDP. PSZ— principal slip zone.**

of the fault gouge, which were all postulated to have occurred due to the frictional heat generated during the earthquake (Fig. 2A). In particular, Boullier et al. (2009) presented a detailed microstructural observation of the fault gouge from the petrographic thin sections, showing the occurrence of random crystallographic grain orientations indicative of an isotropic fabric (Figs. 2B and 2C). The preserved isotropic fabric was proposed by Boullier et al. (2009) to have been derived from thermal pressurization that occurred in the PSZ during the Chi-Chi earthquake.

### GOUGE FABRIC ANALYSIS

We conducted *in situ* neutron texture analysis using bulk fault gouge recovered from core FZ1137, where the core recovery rate was over

99%, to characterize the mineral orientation distribution within the gouge and its heterogeneity within the fault core. We used 12 bulk samples in neutron experiments conducted with the residual stress diffractometer KOWARI (at the Australian Nuclear Science and Technology Organisation, Sydney) (Fig. 2A; Kirstein et al., 2009; Item S1 in the Supplemental Material<sup>1</sup>), which allowed nearly continuous characterization across the fault core including the PSZ. As the main constituent of the samples, illite 1 M was taken to be the mineral most representative of the gouge

<sup>1</sup>Supplemental Material. Methods and supplemental figures. Please visit <https://doi.org/10.1130/GEOL.S.19783141> to access the supplemental material, and contact [editing@geosociety.org](mailto:editing@geosociety.org) with any questions.

fabrics (Hirono et al., 2008). We first measured the illite (020) pole density distribution, then derived the corresponding illite (002) basal pole density figure (Hielscher and Schaeben, 2008) as a measure of c-axis preferred orientation where the pole density is described in units of multiples of a random distribution (MRD) (Fig. 2C; Item S2).

Our fabric intensity data show that the fault gouges have uniformly weak fabrics with an average maximum MRD value of 1.87 and a standard deviation of 0.14. These values are similar to those reported from natural fault gouges collected in the field (Haines et al., 2009). In terms of fabric orientation, two distinguished preferred orientations of the platy illite minerals were found: (1) illite fabric subparallel to parallel to the bedding-parallel fault plane was found in most samples with some scattered pole figures, resembling the background gouge fabric parallel to either the original sedimentary structure and/or the long-term fault shear plane; and (2) illite fabric was found orthogonal to the fault plane and aligned with the slip direction of the Chelungpu fault (i.e., upright and perpendicular to fault strike; Fig. S3C). Notably, sample 10 was oriented anomalously, in keeping with the orientation found in the Chi-Chi PSZ identified by previous studies (Hirono et al., 2008; Ishikawa et al., 2008; Boullier et al., 2009; Chou et al., 2012).

The upright fabric of the gouge can be derived from (1) afterslip folding during gouge consolidation (Haines et al., 2013), (2) shearing along a vertical plane, and (3) development by lateral compaction. Both afterslip folding and shearing along a vertical plane are unlikely, because such deformation is difficult to limit within the PSZ and should also affect the fabric orientations above and below the PSZ, but no upright fabric is observed outside of the PSZ. Therefore, we interpret that the upright fabric of the gouge developed through lateral compaction in response to the local stress orientation.

The compaction at the local scale was likely possible because of the gouge fluidization that occurred locally in the PSZ due to the high coseismic pore fluid pressure caused by thermal pressurization. Because compaction occurs parallel to the maximum principal stress, the upright clay fabric records the maximum principal stress direction right after the Chi-Chi earthquake, which was presumably horizontal in the north-south direction parallel to the strike of the Chelungpu fault. Sample 5 also exhibits an upright fabric similar to that of sample 10, which may provide evidence of another fault strand of the Chi-Chi earthquake or an older event.

### PRESEISMIC AND POSTSEISMIC STRESS

To determine whether the clay fabric indeed records the post-earthquake stress orientation

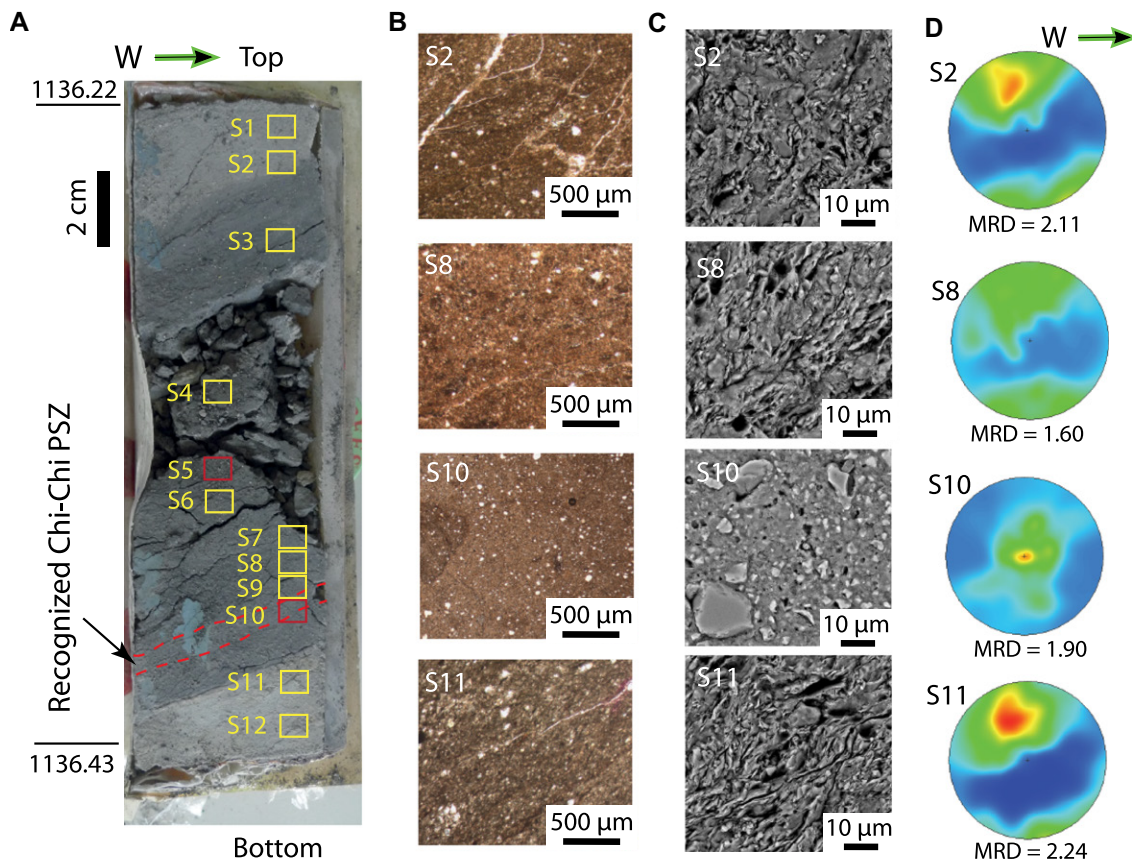


**Figure 2.** The active fault zone of the Chelungpu fault (Taiwan) and its microstructures. (A) Taiwan Chelungpu Fault Drilling Project (TCDP) fault core composed of gray gouge and black gouges. The gouge samples collected for the neutron analysis are marked by yellow boxes on the core. S5 and S10 are shown with red boxes due to different clay fabric orientations. PSZ—principal slip zone. (B,C) Parallel-polarized light observation and backscattered scanning electron microscope images of collected gouge samples. (D) Pole figures of the samples analyzed show two groups of clay fabrics with different orientations. Red color corresponds to maximum multiples of a random distribution (MRD) values, and dark blue corresponds to the minimum MRD values. Maximum MRD values are shown for each pole figure.

of the fault, we infer the gouge stress state after the earthquake by evaluating the pre-earthquake stress state and adding the co-seismic stress change that occurred due to the Chi-Chi earthquake, because no stress measurements have been conducted on the PSZ of the Chelungpu fault to allow direct comparison.

We estimated the direction and relative magnitudes of the pre-earthquake principal stress based on paleostress data derived from the inversion of TCDP core sample fault slip data (Hashimoto et al., 2015). Multiple inversions (using Yamaji's [2000] methods) applied to fault slip data revealed several distinct stress states recorded in the fault slip data, and here we refer to the stress state that represents the most compressive state in the thrust faulting environment. The magnitude of this suggested pre-earthquake stress is further constrained from the overburden stress, frictional strength of the fault gouge, and the assumption that the gouge was critically stressed (Item S3). The resulting stress is shown in Figure 3A, where the maximum principal stress (S1) is 38.1 MPa. Sub-horizontal in the N100°E direction, the intermediate principal stress (S2) is 34.3 MPa, and sub-horizontal in the N10°E direction, the minimum principal stress (S3) is 25.5 MPa and sub-vertical.

We estimated the coseismic stress change based on a two-dimensional (2-D) edge dislocation model (Segall, 2010) of a pure thrust fault.

The dip and the dip direction of the modeled fault was set as 30°E and N110°E, respectively, and a uniform slip along the fault plane was assigned that was adjusted to reproduce the coseismic surface displacements recorded by the global navigation satellite system network (Item S3). The elastic stress change associated with such fault slip was then added to the pre-earthquake stress to obtain the post-earthquake stress state shown in Figure 3A. After the earthquake, stress S1 is 32.1 MPa and subhorizontal in the N20°E direction, S2 is 31.8 MPa and subhorizontal in the N110°E direction, and S3 is 24.9 MPa and subvertical. Comparison of the shear stress resolved onto the fault plane before and after the earthquake suggests that the shear stress drops by ~1.8 MPa. Considering that the TCDP penetrated the fault at ~1 km depth, this is consistent with estimates derived from geodetic data (1–3 MPa; Hsu et al., 2009) and from seismic data (a few mega Pascals; Zhang et al., 2003). As indicated by the orientation of S1 and S2 before and after the earthquake, the maximum principal stress (S1) is perpendicular to the strike of the fault before the earthquake, consistent with the thrust faulting of the Chi-Chi earthquake, but becomes parallel to the strike of the fault after the earthquake. This coseismic stress change is also described in Figure 3B, where the pre- and post-earthquake stress states are described in terms of the horizontal normal

stresses parallel to the dip direction ( $S_{dip}$ ) and the horizontal normal stresses parallel to the strike direction ( $S_{strike}$ ). We compared the stress states with a stress-polygon describing the frictional limits of stress magnitudes in different faulting regimes using a gouge friction of 0.32 constrained from low-velocity experiments (Mizoguchi et al., 2008). The stress state crosses the  $S_{dip} = S_{strike}$  line, indicating the reversal of the maximum horizontal stress direction. These results are consistent with the upright clay fabric observed within the gouge in the principal slip plane. Note that the pre-earthquake stress state we assumed may not be exactly correct, for instance, because the stress may not have been at a critical state or fault zone stress is generally more isotropic than the surrounding host rock (Faulkner et al., 2006). However, the reversal of the S1 and S2 orientation is predicted even if the pre-earthquake stress state is closer to an isotropic state (Fig. 3B).

#### GOUGE FABRIC AS A NEW STRESS INDICATOR

Our results demonstrate that detailed analysis of gouge fabric orientation is an effective method for inferring the post-earthquake stress state on a slip plane that experiences rapid slip. Because thermal pressurization is recognized to be a potentially widespread phenomenon that takes place along seismic faults during

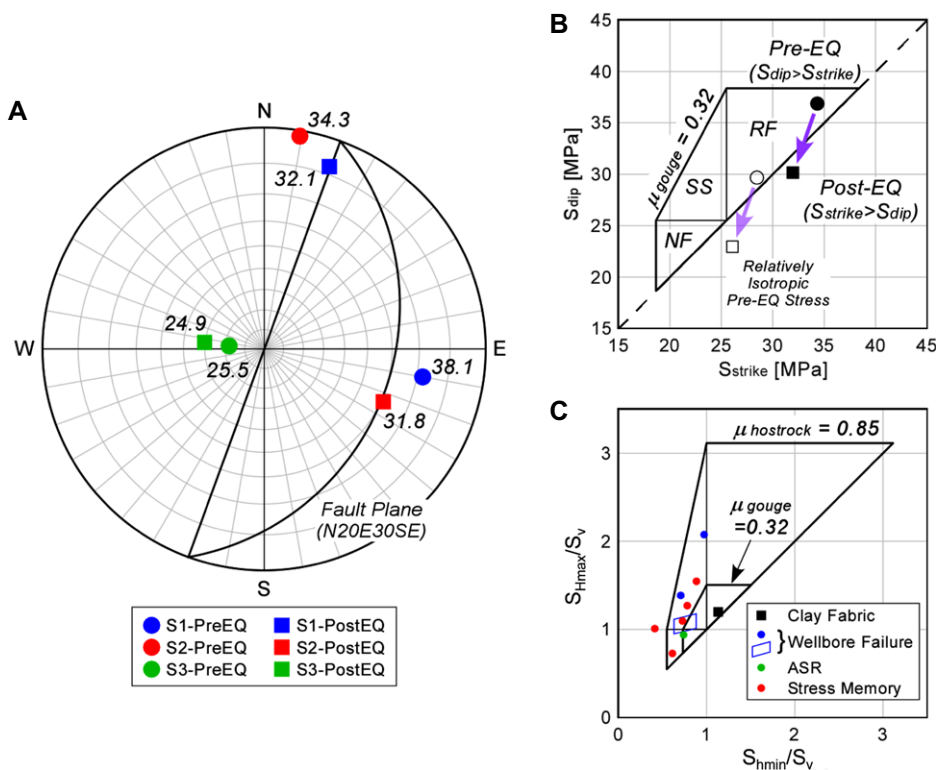


**Figure 3. Stress orientation and magnitude change during the 1999 Chi-Chi earthquake (EQ) in Taiwan. (A) Stereonet plot (lower hemisphere projection) showing the orientations of the principal stresses, before and after the earthquake, constrained in our analysis. The great circle represents the approximate orientation of the Chelungpu fault near the Taiwan Chelungpu Fault Drilling Project (TCDP). (B) Plot of the dip-parallel normal stress,  $S_{dip}$ , and the strike-parallel normal stress,  $S_{strike}$ , before and after the earthquake compared with a stress polygon showing frictional limits of the stress within fault gouge and faulting regimes. Note the crossing of the stress state over the  $S_{dip} = S_{strike}$  line, indicating reversal in the maximum and minimum horizontal stress directions.  $\mu$ —friction; NF—normal fault; SS—strike slip fault; RF—reverse fault. (C) Comparison of the post-earthquake fault stress determined from our analysis of previous stress measurements based on wellbore failure (Lin et al., 2007; Hung et al., 2009; Haimson et al., 2010), anelastic strain recovery (Lin et al., 2006), and stress memory (Yabe et al., 2008) methods. Stress polygons drawn using a gouge friction,  $\mu$ , of 0.32 and host rock friction of 0.85 are based on Byerlee friction (Byerlee, 1978). ASR—anelastic strain recovery.  $S_{Hmax}/S_v$ —ratio of maximum principal horizontal stress over vertical stress;  $S_{Hmin}/S_v$ —ratio of minimum principal horizontal stress over vertical stress.**

earthquakes (Viesca and Garagash, 2015), we expect that similar observations could be made elsewhere to infer post-earthquake stress orientations on faults. A key advantage of using gouge fabric over existing borehole methods is that the stress orientation can be inferred directly on the principal slip plane, which is usually no thicker than a few centimeters (Ma et al., 2006) and is unresolvable using techniques like hydraulic fracturing, observation of wellbore failures, ASR, and overcoring. The stress state on the fault inferred from our fabric analysis and calculations is indeed different from those reported in the literature (Fig. 3C; Lin et al., 2006, 2007; Yabe et al., 2008; Hung et al., 2009; Haimson et al., 2010), which were derived from the application of conventional methods to the host rock. The comparison shows that the host rock is either in a normal or strike-slip faulting regime, whereas the fault plane stress state remained in the reverse fault-

ing regime but with a reversal of orientation of stress S1 and S2.

Our discovery of anomalous clay fabrics, as those shown here, also provides important evidence of the operation of coseismic fault weakening mechanisms. Because the resetting of gouge fabrics can only occur under a fluidized state (Wen and Zhang, 2022), the occurrence of such gouge fabrics suggests that the effective normal fault stress was nearly zero during coseismic slip. Thus, the presence of re-oriented clay fabric provides evidence not only of elevated pore pressure in the fault plane due to thermal pressurization but also of the near-lithostatic pore pressure that was most likely achieved by thermal pressurization. When gouge fluidization is combined with post-earthquake stress states that are not aligned with the pre-existing gouge fabric, the gouge fabric offers a unique opportunity to infer the stress history experienced by the fault during the seismic cycle.

## ACKNOWLEDGMENTS

This research was supported by grants from the Taiwan Republic of China (ROC) Ministry of Science and Technology (MOST 110-2116-M-008-002-MY2) and the Earthquake-Disaster and Risk Evaluation and Management Center of the Ministry of Education (MOE), Taiwan ROC, to Li-Wei Kuo. The neutron diffraction experiments were conducted at the Australia Nuclear Science and Technology Organization's KOWARI beamline (Sydney) through proposal P5385. We thank three reviewers and the editor for their constructive comments.

## REFERENCES CITED

- Brodsky, E.E., and Kanamori, H., 2001, Elastohydrodynamic lubrication of faults: *Journal of Geophysical Research: Solid Earth*, v. 106, p. 16,357–16,374, <https://doi.org/10.1029/2001JB000430>.
- Boullier, A.M., Yeh, E.C., Boutareaud, S., Song, S.R., and Tsai, C.H., 2009, Micro-scale anatomy of the 1999 Chi-Chi earthquake fault zone: *Geochemistry Geophysics Geosystems*, v. 10, Q03016, <https://doi.org/10.1029/2008GC002252>.
- Byerlee, J., 1978, Friction of rocks: *Pure and Applied Geophysics*, v. 116, p. 615–626, <https://doi.org/10.1007/BF00876528>.
- Chou, Y.-M., Song, S.-R., Aubourg, C., Lee, T.-Q., Boullier, A.-M., Song, Y.-F., Yeh, E.-C., Kuo, L.-W., and Wang, C.-Y., 2012, An earthquake slip zone is a magnetic recorder: *Geology*, v. 40, p. 551–554, <https://doi.org/10.1130/G32864.1>.
- Faulkner, D.R., and Rutter, E.H., 2001, Can the maintenance of overpressured fluids in large strike-slip fault zones explain their apparent weakness?: *Geology*, v. 29, p. 503–506, [https://doi.org/10.1130/0091-7613\(2001\)029<0503:CTMOOF>2.0.CO;2](https://doi.org/10.1130/0091-7613(2001)029<0503:CTMOOF>2.0.CO;2).
- Faulkner, D.R., Mitchell, T.M., Healy, D., and Heap, M.J., 2006, Slip on 'weak' faults by the rotation of regional stress in the fracture damage zone: *Nature*, v. 444, p. 922–925, <https://doi.org/10.1038/nature05353>.
- Haimson, B., and Fairhurst, C., 1969, In-situ stress determination at great depth by means of hydraulic fracturing: Berkeley, California, 11<sup>th</sup> U.S. Symposium on Rock Mechanics, abstract ARMA-69-0559.
- Haimson, B., Lin, W., Oku, H., Hung, J.-H., and Song, S.-R., 2010, Integrating borehole-break-out dimensions, strength criteria, and leak-off test results, to constrain the state of stress across the Chelungpu Fault, Taiwan: *Tectonophysics*, v. 482, p. 65–72, <https://doi.org/10.1016/j.tecto.2009.05.016>.
- Haines, S.H., van der Pluijm, B.A., Ikari, M.J., Saffer, D.M., and Marone, C., 2009, Clay fabric intensity in natural and artificial fault gouge: Implications for brittle fault zone processes and sedimentary basin clay fabric evolution: *Journal of Geophysical Research: Solid Earth*, v. 114, B05406, <https://doi.org/10.1029/2008JB005866>.
- Haines, S.H., Kaproth, B., Marone, C., Saffer, D., and van der Pluijm, B., 2013, Shear zones in clay-rich fault gouge: A laboratory study of fabric development and evolution: *Journal of Structural Geology*, v. 51, p. 206–225, <https://doi.org/10.1016/j.jsg.2013.01.002>.
- Hashimoto, Y., Tobe, K., Yeh, E.C., Lin, W., and Song, S.R., 2015, Changes in paleostress and its magnitude related to seismic cycles in the Chelungpu Fault, Taiwan: *Tectonics*, v. 34, p. 2418–2428, <https://doi.org/10.1002/2015TC004005>.
- Hielscher, R., and Schaeben, H., 2008, A novel pole figure inversion method: Specification of the MTEX algorithm: *Journal of Applied*

- Crystallography, v. 41, p. 1024–1037, <https://doi.org/10.1107/S0021889808030112>.
- Hirono, T., et al., 2008, Clay mineral reactions caused by frictional heating during an earthquake: An example from the Taiwan Chelungpu fault: *Geophysical Research Letters*, v. 35, L16303, <https://doi.org/10.1029/2008GL034476>.
- Hsu, Y.-J., Avouac, J.-P., Yu, S.-B., Chang, C.-H., Wu, Y.-M., and Jochen Woessner, J., 2009, Spatio-temporal slip, and stress level on the faults within the western foothills of Taiwan: Implications for fault frictional properties: *Pure and Applied Geophysics*, v. 166, p. 1853–1884, <https://doi.org/10.1007/s00024-009-0510-5>.
- Hung, J.-H., Ma, K.-F., Wang, C.-Y., Ito, H., Lin, W., and Yeh, E.-C., 2009, Subsurface structure, physical properties, fault-zone characteristics and stress state in scientific drill holes of Taiwan Chelungpu Fault Drilling Project: *Tectonophysics*, v. 466, p. 307–321, <https://doi.org/10.1016/j.tecto.2007.11.014>.
- Ishikawa, T., et al., 2008, Coseismic fluid-rock interactions at high temperatures in the Chelungpu fault: *Nature Geoscience*, v. 1, p. 679–683, <https://doi.org/10.1038/ngeo308>.
- Kanamori, H., and Brodsky, E.E., 2004, The physics of earthquakes: *Reports on Progress in Physics*, v. 67, p. 1429–1496, <https://doi.org/10.1088/0034-4885/67/8/R03>.
- Kano, Y., Mori, J., Fujio, R., Ito, H., Yanagidani, T., Nakao, S., and Ma, K.F., 2006, Heat signature on the Chelungpu fault associated with the 1999 Chi-Chi, Taiwan earthquake: *Geophysical Research Letters*, v. 33, L14306, <https://doi.org/10.1029/2006GL026733>.
- Kirstein, O., Luzin, V., and Garbe, U., 2009, The strain-scanning diffractometer Kowari: *Neutron News*, v. 20, p. 34–36, <https://doi.org/10.1080/10448630903241175>.
- Lachenbruch, A.H., and Sass, J.H., 1980, Heat flow and energetics of the San Andreas Fault Zone: *Journal of Geophysical Research: Solid Earth*, v. 85, p. 6185–6222, <https://doi.org/10.1029/JB085iB11p06185>.
- Lin, W., Kwaśniewski, M., Imamura, T., and Matsuki, K., 2006, Determination of three-dimensional in situ stresses from anelastic strain recovery measurement of cores at great depth: *Tectonophysics*, v. 426, p. 221–238, <https://doi.org/10.1016/j.tecto.2006.02.019>.
- Lin, W., Yeh, E.-C., Ito, H., Hung, J.-H., Hirono, T., Soh, W., Ma, K.-F., Kinoshita, M., Wang, C.-Y., and Song, S.-R., 2007, Current stress state and principal stress rotations in the vicinity of the Chelungpu fault induced by the 1999 Chi-Chi, Taiwan, earthquake: *Geophysical Research Letters*, v. 34, L16307, <https://doi.org/10.1029/2007GL030515>.
- Lockner, D.A., Morrow, C., Moore, D., and Hickman, S., 2011, Low strength of deep San Andreas fault gouge from SAFOD core: *Nature*, v. 472, p. 82–85, <https://doi.org/10.1038/nature09927>.
- Ma, K.-F., Brodsky, E.E., Mori, J., Ji, C., Song, T.-R.A., and Kanamori, H., 2003, Evidence for fault lubrication during the 1999 Chi-Chi, Taiwan, earthquake (Mw 7.6): *Geophysical Research Letters*, v. 30, 1244, <https://doi.org/10.1029/2002GL015380>.
- Ma, K.F., et al., 2006, Slip zone and energetics of a large earthquake from the Taiwan Chelungpu-Fault Drilling Project: *Nature*, v. 444, p. 473–476, <https://doi.org/10.1038/nature05253>.
- Mizoguchi, K., Takahashi, M., Tanikawa, W., Masuda, K., Song, S.R., and Soh, W., 2008, Frictional strength of fault gouge in Taiwan Chelungpu fault obtained from TCDP Hole B: *Tectonophysics*, v. 460, p. 198–205, <https://doi.org/10.1016/j.tecto.2008.08.009>.
- Segall, P., 2010, *Earthquake and Volcano Deformation*: Princeton, New Jersey, USA, Princeton University Press, 456 p., <https://doi.org/10.1515/9781400833856>.
- Sibson, R.H., 1973, Interactions between temperature and pore-fluid pressure during earthquake faulting and a mechanism for partial or total stress relief: *Nature*, v. 243, p. 66–68.
- Tanikawa, W., and Shimamoto, T., 2009, Frictional and transport properties of the Chelungpu fault from shallow borehole data and their correlation with seismic behavior during the 1999 Chi-Chi earthquake: *Journal of Geophysical Research: Solid Earth*, v. 114, B01402, <https://doi.org/10.1029/2008JB005750>.
- Viesca, R., and Garagash, D., 2015, Ubiquitous weakening of faults due to thermal pressurization: *Nature Geoscience*, v. 8, p. 875–879, <https://doi.org/10.1038/ngeo2554>.
- Wen, Y., and Zhang, Y., 2022, Evidence of a unique critical fabric surface for granular soils: *Géotechnique*, <https://doi.org/10.1680/jgeot.21.00126>.
- Yabe, Y., Song, S.R., and Wang, C.Y., 2008, In-situ stress at the northern portion of the Chelungpu fault, Taiwan, estimated on boring cores recovered from a 2-km-deep hole of TCDP: *Earth and Planetary Science Letters*, v. 60, p. 809–819, <https://doi.org/10.1186/BF03352832>.
- Yamaji, A., 2000, The multiple inverse method; a new technique to separate stresses from heterogeneous fault-slip data: *Journal of Structural Geology*, v. 22, p. 441–452, [https://doi.org/10.1016/S0191-8141\(99\)00163-7](https://doi.org/10.1016/S0191-8141(99)00163-7).
- Zhang, W., Iwata, T., Irikura, K., Sekiguchi, H., and Bouchon, M., 2003, Heterogeneous distribution of the dynamic source parameters of the 1999 Chi-Chi, Taiwan, earthquake: *Journal of Geophysical Research: Solid Earth*, v. 108, 2232, <https://doi.org/10.1029/2002JB001889>.
- Zoback, M.D., Barton, C.A., Brudy, M., Castillo, D.A., Finkbeiner, T., Grollmund, B.R., Moos, D.B., Peska, P., Ward, C.D., and Wiprut, D.J., 2003, Determination of stress orientation and magnitude in deep wells: *International Journal of Rock Mechanics and Mining Sciences*, v. 40, p. 1049–1076, <https://doi.org/10.1016/j.ijrmms.2003.07.001>.

Printed in USA